A review: microstructure and properties of Tin-Silver-Copper lead-free solder series for the applications of electronics

Muhammad Aamir, Riaz Muhammad, Majid Tolouei-Rad, Khaled Giasin, Vadim V. Silberrchmidt

Abstract

Purpose - The research on lead-free solder alloys has increased in past decades due to awareness of the environmental impact of lead contents in soldering alloys. This has led to the introduction and development of different grades of lead-free solders alloys in the global market. Tin-Silver-Copper is a lead-free alloy which has been acknowledged by different consortia as a good alternative to conventional Tin-Lead alloy. The purpose of this review is to provide comprehensive knowledge about the Tin-Silver-Copper series.

Design/methodology/approach – The approach of this study reviews the microstructure and some other properties of Tin-Silver-Copper Series after the addition of Indium, Titanium, Iron, Zinc, Zirconium, Bismuth, Nickel, Antimony, Gallium, Aluminium, Cerium, Lanthanum, Yttrium, Erbium, Praseodymium, Neodymium, Ytterbium, Nanoparticles of Nickel, Cobalt, Silicon carbide, Aluminium oxide, Zinc oxide, Titanium dioxide, Cerium oxide, Zirconium oxide, and Titanium diboride as well as Carbon nanotubes, Nickel-coated carbon nanotubes, single-walled carbon nanotubes and Graphene-nano-sheets.

Findings – The current paper presents a comprehensive review of the Tin-Silver-Copper solder series with possible solutions for improving their microstructure, melting point, mechanical properties, and wettability through the addition of different elements/nanoparticles and other materials.

Originality/value - This paper summarizes the useful findings of the Tin-Silver-Copper series comprehensively. This information will assist in future work for the design and development of novel lead-free solder alloys.

Keywords: Tin-Silver-Copper series; Alloying Element; Melting Point; Microstructure; Mechanical Properties; Wettability

Paper Type: Review Paper

1. Introduction

Soldering is the process of joining two or more metals by means of a third metal or an alloy with a relatively lower melting point (MP) (Efzan and Marini, 2012). Solder joints are primarily and extensively used to physically hold assemblies together, allowing contraction and expansion of different components, dissipating any generated heat and transmitting electrical signals. Therefore, the reliability of a solder joint depends on the performance and quality of the solder alloys (Aamir *et al.*, 2015). In the early era of the microelectronics industry, Tin-Lead *(Sn_{63}-Pb_{37})* was the most commonly used solder alloy in to attach electrical and electronic equipment to printed circuit boards (Ma and Suhling, 2009). This was due to their combined merit of low cost and better mechanical, metallurgical and physical properties, mainly facilitated by the Lead *(Pb)* content (Lee, 1997). However, *Pb* has restrictions in its utilization in electronics through legislation worldwide due to environmental concerns and the low recycling rate of electronics (Cheng *et*

al., 2017). Therefore, electronic manufacturers require a suitable lead-free solder *(LFS)* which is more reliable for soldering joints and is environmentally benign (Lee, 1997).

Generally, few families of *LFS* alloys are well-acknowledged and prevailing choices in electronic industries. Amongst them, the most popular *LFS* alloy is the Tin-Silver-copper (*SAC)* series (Aamir *et al.*, 2017a; Aamir *et al.*, 2017b). A survey has shown that almost 70% of accepted lead-free solders *(LFSs)* are *SAC* alloys due to their good properties compared to other eutectic alloys (Shnawah *et al.*, 2012). In addition, the *SAC* series provides better mechanical support in electronic devices because of its good joint strength (Harrison *et al.*, 2001).

In *SAC*, the near eutectic composition consists of a high volume of *β*-Tin *(Sn)* matrix and intermetallic compounds *(IMCs)* namely Ag_3Sn, Cu_6Sn_5 and Cu_3Sn (El-Daly *et al.*, 2013). In comparison to the *Sn*-matrix, *IMCs* are brittle in nature and represent the properties of solder alloys (Sadiq *et al.*, 2013). It is worth noting that the formation of Ag_3Sn is due to the reaction between *Sn* and Silver *(Ag)* whereas Cu_6Sn_5 is possibly formed by the reaction between *Sn* and Copper *(Cu)*. No reaction has been found between *Ag* and *Cu* for the formation of any types of *IMCs* (Vianco and Shangguan, 2006). It has also been reported that Cu_3Sn does not form at the eutectic point unless the content of *Cu* is high enough for its formation at high temperature (Ma and Suhling, 2009). *Cu* additions in the *SAC* series improve their wettability and lower their melting temperature (Nimmo, 2004). Furthermore, higher *Ag* contents in the *Sn*-rich matrix yield a higher amount of Ag_3Sn which may result in higher strength. However, high *Ag* contents with high elastic modulus *(E)* and yield strength *(YS)* show reasonably low ductility (Che *et al.*, 2010).

In spite of being acknowledged *LFSs*, the *SAC* series still has some problems such as high *MP*, poor wettability and coarser microstructures (Sadiq *et al.*, 2013). To overcome these problems and to further improve the properties of *SAC* for the reliability of solder joints, different elements and micro or nanoparticles are added to the *SAC* which changes the microstructure and enhances other properties (Sona and Prabhu, 2013). Therefore, in this review, the impact of adding different elements/nanoparticles or other materials on the *MP*, microstructure, mechanical properties and wettability on all *SAC* family members are presented.

2. Melting Point

Melting temperature *(MT)* is one of the important properties for the development of *LFSs* (El-Daly and Hammad, 2012). *MT* is the liquidus temperature *(T_L)* making the solder alloy completely molten which is necessary for soldering operations (Abtew and Selvaduray, 2000). *MT* is essential to develop better solder joints and occurs if the solidus temperature *(T_S)* is low (Mei *et al.*, 1996) because rapid solidification can provide better and refined microstructure which has a direct impact on solder joint's strength (Kanlayasiri *et al.*, 2009). Moreover, a good solder alloy should have a narrow melting range *($\Delta T = T_L - T_S$)* and low *MT* (El-Daly and Hammad, 2012). Taking into account that a conventional eutectic *Sn-Pb* solder melts at 183°C, this should be considered as a benchmark for all new *LFSs* (Jeon *et al.*, 2008), However, the *MP* of *SAC* is 217°C which results in thicker *IMCs* than that of *Sn-Pb*. Therefore, some

researchers have added alloying elements or nanoparticles to reduce the *MT* of the *SAC* series. For instance, (Kanlayasiri *et al.*, 2009) reported that the doping of Indium (*In*) into *SAC* lowers the T_S and T_L. Their results conclude that upon addition of 3 wt% *In* to *SAC,* T_S (219.4 ºC) and T_L (241.7 ºC) decrease by 21.7 ºC and 11.5 ºC, respectively. Subsequently, the difference between T_S and T_L of the *SAC* increased from 22.3 °C to 32.5 °C. However, *In* is expensive and its high cost increases the cost of *LFSs.* (Chuang *et al.*, 2012) investigated the influence of Titanium *(Ti)* on the *MT* of *SAC*. Their results show that the addition of 1.0 wt% of *Ti* into *SAC* decrease the T_S and T_L from 216.92 ºC and 221.58 ºC to 216.59 ºC and 219.47 ºC, respectively. In addition, the melting range of *SAC* also decreased from 4.66 ºC to 2.88 ºC. It is worth noting that the narrow melting range is one of the desirable thermal properties of solders, meaning that solders exist in the liquid form only for a very short time during solidification for the formation of acceptable joints. In another study by (Shnawah *et al.*, 2013), differential scale calorimetry (*DSC)* analysis was carried out to check the thermal behaviour of *SAC* after the addition of different compositions of Iron (*Fe).* They found that 0.6 wt% of *Fe* gave a lower *MP* by showing one endothermic peak at 221.35 ºC at a eutectic composition. (Huang and Wang, 2005) also reported a decrease in the *MP* of *SAC* upon addition of Bismuth (*Bi)*. According to their findings, the T_S of *SAC-2Bi* and *SAC-4Bi* were 213.08 ºC and 206.40 ºC, respectively. However, peeling of the solder joint appeared when the addition *Bi* was more than 4 wt%.

Furthermore, the addition of Rare-Earth (*RE)* elements (Wu and Wong, 2007) and nanoparticles (Efzan Mhd Noor *et al.*, 2013) have also contributed in *SAC* series to give better properties but have not drastically affected the *MP*. For instance, (Dudek and Chawla, 2010) studied *DSC* curves of *SAC* and *SAC-0.5RE*. Their selected *RE* elements were Lanthanum *(La),* Cerium *(Ce),* Yttrium *(Y)*, where it was found that all solders *(La, Ce, and Y)* displayed a single endothermic peak between 217 ºC and 219 ºC. (Ping Liu *et al.*, 2008) studied that minor addition of Silicon carbide (*SiC)* nanoparticles to the *SAC* did not change its *MT* noticeably. However, upon the addition of only 0.2 wt% *SiC*, a lower *MP* value was observed as the endothermic peak shifted from 219.9 ºC to 218.9 ºC. (Tsao *et al.*, 2013) analysed *DSC* curves of the *SAC* doped with Aluminium oxide (Al_2O_3) nanoparticles. It was found that the *MP* of *SAC,* which was 221.2 ºC, slightly increased as the amount of Al_2O_3 nanoparticles increased. (Gain *et al.*, 2011) also observed no significant change in the *MP* of SAC with 1 wt% *of Titanium dioxide* (TiO_2) nanoparticles. It was concluded that *DSC* analyses gave only a eutectic peak from 217 ºC to 217.64 ºC. Similar behaviour was noted in another study by (Chang *et al.*, 2011). In conclusions, adding alloying elements and nanoparticles to *SAC* series have little effect on the *MT*. However, in future research, it will be necessary to ensure that the addition of the fourth element or nanoparticles can slightly influence the *MP* of *SAC* series.

3. Microstructure

A thin layer of *IMCs* is required to attain a better metallurgical bond for the reliability of electronic solders; however, their higher growth has undesirable impacts on mechanical properties due to their brittle nature (Liang *et al.*, 2014). Therefore, it is important to expand the knowledge of *IMCs* for the reliability of solder

interconnections (Aamir *et al.*, 2017c; Aamir *et al.*, 2019). This brief review notes how the addition of alloying elements or composite approach into *SAC* series is discussed to highlight the impact of participates in suppressing the growth of *IMCs* for refined and uniform microstructures.

In the experiments conducted by (Chuang *et al.*, 2012), It was concluded that after the addition of different composition of *Ti* into *SAC,* the microstructure of *SAC* become uniform due to active properties of *Ti*, which gives rise to heterogeneous *IMCs* and reduces the dendritic size. However, it was recommended that the *Ti* concentration should not exceed greater than 1.0 wt% which in return gives rise to coarse Ti_2Sn_3 in the eutectic colonies and makes the microstructure of *SAC* worse. (Sabri *et al.*, 2013) found that inclusions of Aluminium (*Al)* in *SAC* leads to the arrangement of large amount of additional Ag_3Al and Al_2Cu *IMCs*. These *IMCs* posses snowflake, circle, rod, and quadrangle shaped morphologies and were lightly distributed within the microstructures located in and at the vicinity of interdendritic regions. Moreover, these additional *IMCs* refined the microstructure of *SAC* by restraining the growth formation of *IMCs* (Ag_3Sn and Cu_6Sn_5). In another study by (Leong and Haseeb, 2016) the minor addition of *Al* into *SAC* on the interfacial structure between solder and copper substrate during reflow was investigated. It was determined that minor addition of *Al* into *SAC* formed small equiaxed *Cu-Al* particles known as Cu_3Al_2, which suppressed the growth of the interfacial Cu_6Sn_5 *IMC* after reflow. (Zhang *et al.*, 2012a) investigated doping of Zinc (*Zn)* into *SAC* remarkably refined the microstructure with the condition that concentrations of *Zn* should be limited to 0.8 wt%. The refinement in microstructure is due to the formation of dispersed *Cu-Zn IMCs* which reduces the thickness of *IMCs* and ultimately changes the morphology. (Hammad, 2013) found that adding 0.05 wt% *Ni* into *SAC* formed $(Cu,Ni)_6Sn_5$ *IMCs* in the eutectic regions, which decreased the inter-particle spacing and resulted in a more refined morphology. (Hongxuan Wang *et al.*, 2019) fabricated *SAC* with 0.2 wt% Zirconium *(Zr)* by vacuum induction melting method. Their study demonstrates that *Zr* refines the microstructure of *SAC* by reducing the size of *IMCs* which further participates in the improved strength of the solder alloy. Moreover, *0.2Zr* wt% significantly gave better results even at isothermal aging. However, no change in the melting range was observed.

RE elements are greatly acknowledged as a good surface-active agent and are considered vital for materials to improve their microstructure and mechanical properties (Sadiq *et al.*, 2013). These elements can accumulate at the grain/dendrite boundaries and can lower the energy of the grain/dendrite boundary by restricting the motion of the boundaries. Thus, restricting the growth of *IMCs* and giving a refined microstructure (Xia *et al.*, 2002). (Dudek and Chawla, 2010) reported that *RE* addition into *SAC* produced *RE*-containing particles i.e. $RESn_3$ *IMC* apart from Cu_6Sn_5 and Ag_3Sn which were responsible for the refinement of the microstructure as shown in Figure 1.

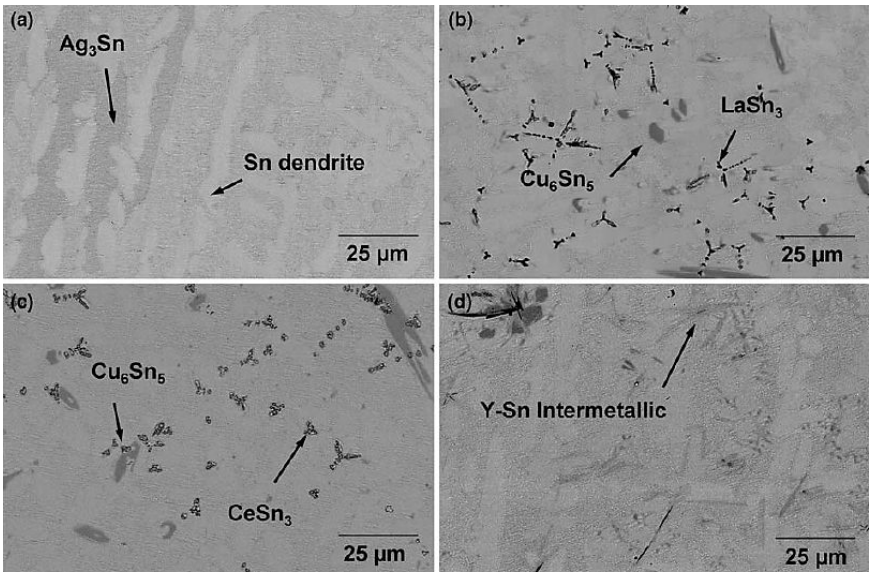

Figure 1: *SEM* micrographs of (a) *SAC* with the addition of 0.5 wt% of (b) *La* (c) *Ce* and (d) *Y* (Dudek and Chawla, 2010)

In addition, (Yasmin and Sadiq, 2014) have concluded that the appropriate composition of *La* in *SAC* reduces the grain size and provides better microstructure by effectively suppressing the growth rate of *IMCs (*Ag_3Sn *and* Cu_6Sn_5*)* even during thermal ageing. This refinement in the microstructure of *SAC* was due to the aggregation of *La* at the interface which provided blockage for the production of large *IMCs*. The same recommendation was made in another study by (Sadiq *et al.*, 2013). Moreover, a careful examination of the microstructure after *Ce* inclusion in *SAC* has been done by (W Chen *et al.*, 2011). Their results showed that the addition of *Ce* promoted the formation of *Ce-Sn IMCs* which acted as a blockage to decrease the growth of Ag_3Sn and Cu_6Sn; thus, giving a refined microstructure. (Zhang *et al.*, 2012b) have also studied the contribution of 0.03 wt% *Ce* in *SAC*. Their study showed that the activation energy for the growth of *IMCs* was higher for *Ce* based *SAC* which was responsible for reducing the growth of *IMCs* and increasing the strength of the solder joint. Furthermore, (Tu *et al.*, 2017) have reported that 0.15 wt% of *Ce* addition into *SAC* improved microstructure by reducing the thickness of the *IMC*s. (Zhang *et al.*, 2014) have recommended that additions of 0.05 wt% of Ytterbium (*Yb)* in *SAC* improves the properties of *SAC* in electronic packaging and refines the microstructure by retarding the growth of *IMCs* during soldering. In another study by (Gao *et al.*, 2010b), the incorporation of a small concentration of Praseodymium (*Pr)* in *SAC* has shown to produce extra $PrSn_3$ particles which restrict the *IMCs* growth because of the heterogeneous nucleation by lowering the reaction time of liquid solder with the substrate. However, more than 0.05 wt% of *Pr* resulted in the arrangement of bulk $PrSn_3$ compound.

Nanoparticles also play a vital role in changing the microstructure of *SAC* series. For instance, (Ping Liu *et al.*, 2008) concluded that inclusion of 0.05 wt% *SiC* nanoparticles remarkably decreased the average grain size due to the strong adsorption effect and high surface free energy which led to the refined *IMCs.* (Sharma *et al.*, 2019) used the simple mechanical blending and casting method to add Zirconium oxide (ZrO_2*)* nanoparticles into the *SAC*. It was concluded that after the addition of ZrO_2 nanoparticles, the

thickness of the grain size, and *IMCs* such as Ag_3Sn and Cu_6Sn_5 were refined by 46, 14, and 26%, respectively in comparison to the original *SAC* alloy. (Bashir *et al.*, 2016) have used nanoparticles doped flux technique to add 2 wt% *Co* nanoparticles into *SAC*. The influence of *Co* nanoparticles doped flux was then investigated in an electro-migration *(EM)* test which was performed in an oil batch maintained at a constant temperature of 80 ºC for a maximum duration of 1128 h with a current density of 1 × 104 A/cm^2. Their study concluded that the presence of 2 wt% *Co* nanoparticles into *SAC* restricted the size of *IMCs* both at the cathode and anode side. In addition, the tensile strength of the solder joint also increased after the addition of *Co* nanoparticles when *EM* test was performed at 150 ºC for 0 h and 192 h. This study showed that 2 wt% *Co* nanoparticles doped flux improve the reliability of *SAC* solder joints. (Sujan *et al.*, 2017) also worked on the addition of *Co* nanoparticle by flux doping technique. This method is useful in the surface mount and technology and does not require any further steps in the manufacturing line. Their results have shown that the addition of *Co*-nanoparticles with an average size of 58 nm into *SAC* stabilized the formation of Cu_6Sn_5 *IMC* and improved the growth of *Co* containing *IMCs*. (Haseeb *et al.*, 2017) have provided an overview to discuss the effects of metallic nanoparticles on the characteristics of interfacial *IMCs* in *Sn*-based solder joints on *Cu* substrates during reflow and thermal aging. The nanoparticles of *Ni, Co, Zn, Mo, Mn,* and *Ti* were mechanically blended with the *SAC* solder paste. It was shown that through the paste mixing route the *Ni, Co, Zn,* and *Mn* nanoparticles greatly contributed in changing the morphology and reducing the thickness of *IMCs* which helped the solder joint to perform in a favourable way. (Basak *et al.*, 2018) investigated the addition of a minor amount of *Fe or* Al_2O_3 nanoparticles into *SAC.* Their results indicated that supplements of *Fe* nanoparticles formed $FeSn_2$, together with the *IMCs* of *SAC* alloy i.e. Ag_3Sn and Cu_6Sn_5, which stopped the growth of grains/*IMCs* during aging/reflowing. However, Al_2O_3 nanoparticles did not participate in phase formation but acted as a grain refiner. (Yakymovych *et al.*, 2017) added *Ni* nanoparticles into *SAC* using a cold-pressing method in which powders of *SAC* and *Ni* nanopowders were mixed mechanically, and processed into 8 mm diameter rods. It was observed that the presence of *Ni* nanoparticles in *SAC* formed a $(Cu, Ni)_6Sn_5$ phase which participated in the refinement of the microstructure due to the fine distribution of *IMCs* in the *Sn* matrix. (Gain and Zhang, 2019) also studied that 0.5 wt% *Ni*-nanoparticles into *SAC* produced a new *(Cu, Ni)-Sn IMC* phases as shown in Figure 2. The new phase of *IMC* refined the microstructure of *SAC* and improved the mechanical reliability of electronic interconnections which subsequently, enhanced the lifespan of miniaturized electronic products.

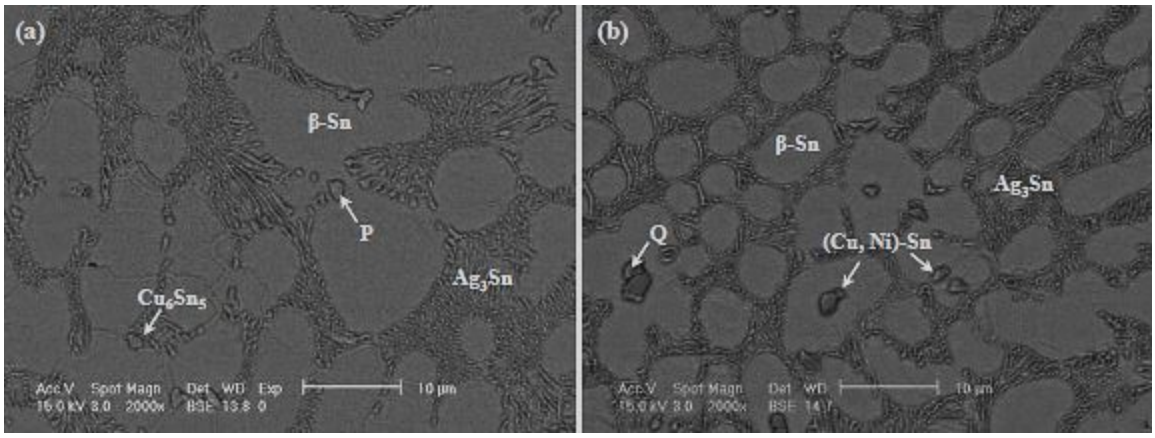

Figure 2: *SEM* images of (a) *SAC* and (b) SAC-0.5wt% nanosized *Ni* particles (Gain and Zhang, 2019)

Carbon nanotubes *(CNTs)* have been acknowledged as giving better physical, electrical and mechanical properties which make them suitable for the fabrication of novel composites (Nai *et al.*, 2008). (Zhu *et al.*, 2018) worked on doping of *CNTs* into *SAC* with three different ranges of diameter 10-20, 40-60, and 60-100 nm presented in Figure 3. Their studies conclude that the addition of *CNTs* in *SAC* provides better performance. Among all, the addition of *CNTs* in *SAC* in the range of diameter (40-60 nm) produced a refined microstructure by lowering the growth rate of *IMCs* up to 30.9%. The refinement in microstructure was attributed due to the agglomeration and adsorption of *CNTs* in the solder matrix and *IMCs* interfacial.

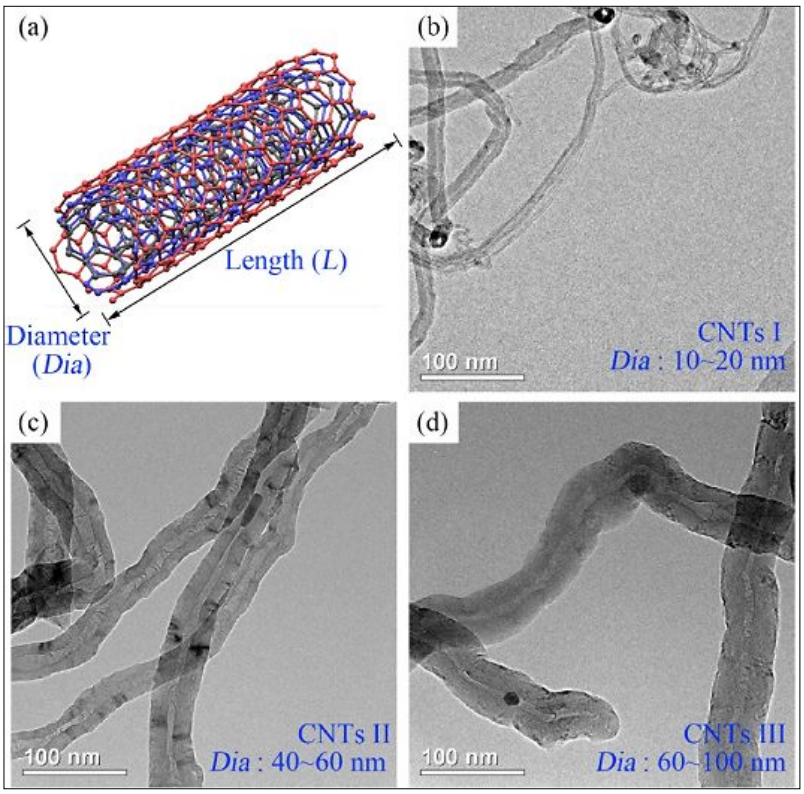

Figure 3: (a) Schematic diagram of *MWCNTs* structure, and *TEM* images of *CNTs*: (b) 10~20 (c) 40~60nm (d) 60~100 (Zhu *et al.*, 2018).

(Kumar *et al.*, 2008) have concluded that adding single-walled carbon nanotubes (*SWCNT)* into *SAC* plays a significant role in reducing the average size of *IMCs* due to the dispersion of nanotubes at the grain boundaries of Ag_3Sn, which results in uniform morphology. (Xu *et al.*, 2015) have studied the impact of Graphene-nano-sheets (*GNSs)* on *SAC*. Their study found that *GNSs* participated in restricting grain growth and gave fine *IMCs.* The average size of the *IMCs* after the addition of 0.03, 0.07, and 0.10 Wt% *GNSs* reduced to 1.35, 1.24 and 1.21 μm, respectively, compared to1.96 μm of *SAC*. All These reduced sizes of *IMCs* play a vital role to enhance the reliability of solder joints.

Overall, the addition of appropriate composition of alloying elements, nanoparticles and composites can significantly change the microstructure of *SAC* series. However, the addition of more than a critical composition can further deteriorate the properties of the solder joint. Therefore, it is highly recommended to select the optimum doping concentrations.

4. Mechanical properties

Alloying elements and nanoparticles also play a significant role in the improvement of mechanical properties of *SAC* series (Sun and Zhang, 2015). Table 1 shows the impact of adding alloying elements, nanoparticles or other materials on the mechanical properties of *SAC*.

Table 1: Role of the fourth element in the mechanical properties of *SAC*

Alloying element	Composition wt%	Mechanical properties	References
Ti	Up to 1.0 wt%	Increase the *YS, UTS,* and microhardness of *SAC*	(Chuang *et al.*, 2012)
Fe	0.6 wt%	Shear strength of *SAC* increases up to 53 MPa from 29 MPa	(Fallahi *et al.*, 2012)
Zn	0.8 wt%	Improves the tensile force of *the SAC* joint by 10%.	(Zhang *et al.*, 2012a)
Ni	0.5 wt%	Improves *YS*, *UTS,* and ductility of *SAC*	(El-Daly and El-Taher, 2013)
Sb	0.5 wt%	Gives higher strength and ductility	(Hammad, 2018)
Ga	Up to 0.5 wt%	Improves the shear strength of *SAC* solder joint up to 17.9%	(Luo *et al.*, 2014)
La	0.3 wt%	Increase in *YS*, *UTS*, and ductility are found which then improve toughness, creep and fatigue resistance of the *SAC*	(Ali, 2015)
Y	<0.15 wt%	The strength of the *SAC* joint is improved	(Hao *et al.*, 2007)
Er	≤0.1 wt%	Shear strength of *SAC* solder is improved by 18%	(Shi *et al.*, 2008)

Nd	0.05 wt %	Pull force and shear force of *SAC* joint are increased by 19.4% and 23.6%, respectively	(Gao *et al.*, 2010a)
Pr	0.05 wt%	Improves pull force and shear force of *SAC* solder	(Gao *et al.*, 2010b)
Yb	Up to 0.05 wt%	The tensile force of the *SAC* solder joint increase by 25.4%	(Zhang *et al.*, 2014)
Ce	0.15 wt%	Increase the shear strength, ductility, *E, YS,* and *UTS*	(Tu *et al.*, 2017)
Al Nanoparticles	3.0 wt%	Improves the shear strength of *SAC*	(Gain *et al.*, 2010)
Al_2O_3 *Nanoparticles*	1.0 wt%	The shear strength after 1 cycle and 8 cycles of reflow is increase by 14.4% and 16.5%	(Tsao *et al.*, 2013)
TiO_2 *Nanoparticles*	0.1 wt%	Gives better microhardness and tensile properties	(Tang *et al.*, 2014)
CeO_2 *Nanoparticles*	0.75 wt%	improves *YS* and *UTS* of *SAC*	(Roshanghias *et al.*, 2012)
TiB_2 *Nanoparticles*	3 vol%	Increase *YS* and *UTS* by 26% and 23%, respectively	(Nai *et al.*, 2006)
Co- nanoparticles	2 wt%	Increase the tensile strength of *SAC*	(Bashir *et al.*, 2016)
Ni- nanoparticles	0.5 wt%	The elastic modulus, shear modulus, and microhardness increase by 8%, 11.2%, and 16.7% in *SAC*, respectively.	(Gain and Zhang, 2019)
Ni-CNTs	0.05 wt%	Improves the tensile strength of *SAC* solder slabs and joints	(Yang *et al.*, 2014)
SWCNT	1.0 wt%	Increase the *UTS* of *SAC* up to 50%	(Kumar *et al.*, 2008)
MWCNT	10-60 nm	Improvement *E, YS* and *UTS* of *SAC* are found	(Zhu *et al.*, 2018)
GNSs	0.03 wt%	Increase the *UTS* of *SAC* solder by approximately 10%	(XD Liu *et al.*, 2013)

(Chuang *et al.*, 2012) have investigated that up to 1.0 wt% of *Ti* in *SAC* improves the mechanical properties of *SAC.* Their study also concludes that excess concentrations of *Ti* produce coarse Ti_2Sn_3 in the eutectic colonies which subsequently, degrades the mechanical properties of *SAC*. (Fallahi *et al.*, 2012) have examined that adding 0.2 wt% and 0.6 wt% of *Fe* increases the shear strength of *SAC* up to 40 MPa and 53 MPa, respectively. (Zhang *et al.*, 2012a) have concluded that the addition of 0.8 wt% of *Zn* increases the strength of the *SAC.* However, more than 0.8 wt% of *Zn* gave disperse *Cu-Zn IMCs* which resulted in coarsening of the microstructure because of the great affinity of *Zn* towards oxygen. Therefore, excessive *Zn* contents result in the formation of ZnO_2 which untimely reduce the tensile strength. (El-Daly and El-Taher, 2013) have reported that *YS*, *UTS,* and ductility of the *SAC* are improved

after the addition of 0.05 wt% of *Ni* because of the refined microstructure. However, addition of 0.1 wt% of *Ni* into *SAC* resulted in abrasive microstructure which in turns degraded the mechanical properties. (GY Li *et al.*, 2006; BL Chen and Li, 2004) have found in their studies that doping of *Sb* also improves the tensile strength of *SAC*. This improvement in strength was due to the redcued size of IMCs which ultimately refined the microstructure. The same investigation was articled by (Hammad, 2018) who recommended 0.5 wt% of *Sb* into *SAC* for improving the mechanical strength and ductility of the solder joint. In another study by (Luo *et al.*, 2014), the addition of up to 0.5 wt% of *Ga* is recommended to improve the shear strength of *SAC* by 17.9%.

Regarding *RE* elements, (Ali, 2015) has concluded that the optimum *La* concentration in *SAC* for desired mechanical properties including *YS, UTS,* and ductility is 0.3 wt%. (Aamir *et al.*, 2017b) reported that better mechanical properties can be obtained when *La* composition is less than 0.4 wt% even at thermal ageing. (Hao *et al.*, 2007) found improvement in the strength of *SAC* after the addition of *Y*; however, the joint strength decreased dramatically beyond 0.15 wt% of *Y* concentrations. (Shi *et al.*, 2008) reported that adding ≤0.1 wt% *Er* to *SAC* increases the shear strength significantly due to reduced size of Ag_3Sn and Cu_6Sn_5. (Gao *et al.*, 2010a) concluded that when the *Nd* supplement was 0.05 wt%, the pull force and shear force of the solder joint was improved by 19.4% and 23.6%, respectively. The improvement in pull force and shear force was due to the refinement in the *IMCs* by *Nd*. Their study also suggested that amount of *Nd* in *SAC* should not exceed 0.25 wt% . In another study by (Gao *et al.*, 2010b) addition of up to 0.05 wt% of *Pr* also increased both pull force and shear force by 18.5% and 19.4%, respectively. Similarly, (Zhang *et al.*, 2014) reported that inclusions of 0.05 wt% *Yb* to the *SAC* increase the tensile force of *SAC* solder joint by 25.4%. (Tu *et al.*, 2017) concluded that addition of 0.15 wt% of *Ce* into *SAC* improved *E, YS* and *UTS* of *SAC.* Furthermore, *SAC-0.15Ce* also gave better shear strength even after thermal ageing as shown in Figure 4.

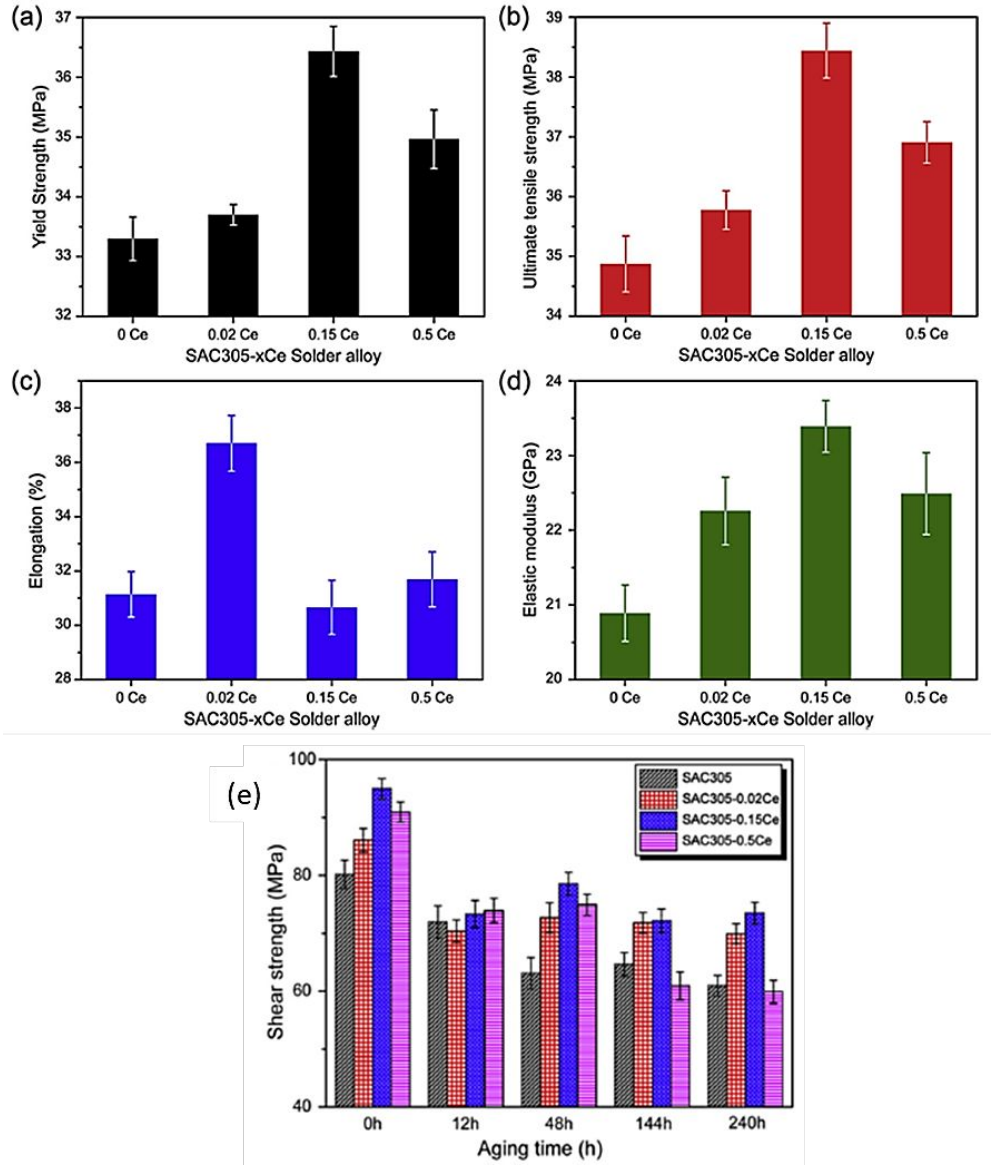

Figure 4: Mechanical properties of the *SAC* with different compositions of *Ce* (Tu *et al.*, 2017)

(Tsao *et al.*, 2013) concluded that the addition of 1 wt% of Al_2O_3 nanoparticles increased the shear strength of *SAC* after 1 cycle and 8 cycles of reflow by 14.4% and 16.5%, respectively. (Tang *et al.*, 2014) added different compositions of TiO_2 nanoparticles into *SAC* which improved the mechanical properties at 0.1 wt% of TiO_2 nanoparticles into *SAC*. The improvement was due to the refinement of the microstructure after the reduced space between the Ag_3Sn *IMCs*. (Bashir *et al.*, 2016) concluded that 2 wt% Co nanoparticles doped flux improved the reliability of *SAC* solder joint because the tensile strength of the solder joint increased after 0 h as well as 192 h of *EM* test conducted at 150 °C. (Gain and Zhang, 2018) have reported that adding 1.0 wt% of TiO_2 nanoparticles into *SAC* prepared by mixing process enhances the creep and shear strength. It was also noted that Cu_6Sn_5 and Cu_3Sn phases were observed on *Cu* substrate through interfacial structure characterization, and a ternary *(Cu, Ni)-Sn* phase was grown on *Au/Ni*-plated *Cu* pad Ball Grid Array electronic interconnect system. These *IMCs* started growing

during thermal aging, however, TiO_2 nanoparticles suppressed the growth of these *IMC*s and thus, the creep, shear strength, and thermal shock resistance were improved. (Gain and Zhang, 2019) have investigated that in addition to the improvement in electrical properties, the elastic modulus, shear modulus, and microhardness are also improved by 8%, 11.2%, and 16.7%, respectively, when the addition of *Ni*-nanoparticles into *SAC* is 0.5 wt%. The reason of overall good properties of the solder joints is the appearance of relatively fine *IMCs* dispersed in *β-Sn* matrix and the fine microstructure. (Roshanghias *et al.*, 2012) have recommended that the best combination of mechanical properties is achieved with 0.75 wt% of CeO_2 nanoparticles into *SAC*. (Nai *et al.*, 2006) suggested that 3 vol% of Titanium diboride (TiB_2) nanoparticles resulted in improved levels of *YS* and *UTS* by 26% and 23%, respectively. (Yang *et al.*, 2014) concluded that 0.05 wt% *Ni*-coated carbon nanotubes (*Ni-CNTs)* into *SAC* significantly improved the tensile strength. The prime cause in its better tensile strength is due to the *CNTs* which obstruct the start of dislocation motion in the *SAC*. (Kumar *et al.*, 2008) concluded that 1.0 wt% of *SWCNT* enhanced the *UTS* of *SAC* up to 50%. (Zhu *et al.*, 2018) also found that the reinforcement of *CNTs* in *SAC* improved *E, YS*, and *UTS*. The recommended range of the diameter of *CNTs* is 40-60 nm which contributed to reducing the growth of *IMCs* and thus, provides superior mechanical properties. Furthermore, upon addition of 0.03 wt% of *GNSs*, the *UTS* of *SAC* was improved approximately by 10%, because of the refined microstructure due to the reduced average size of *IMCs* (XD Liu *et al.*, 2013). Overall, the alloying elements and nanoparticles significantly contributed in the refinement of microstructure and improved mechanical properties of *SAC* series. However, it should be noted that there is an appropriate concentration beyond which those properties degrade.

5. Wettability

Wettability is used to examine the wetting properties that include surface tension and wetting force (Sadiq, 2012). Traditional *Sn-Pb* solder owns better wettability due to the presence of *Pb* (Dharma *et al.*, 2009; Wu *et al.*, 2004). Thus, when changing from *Sn-Pb* to *LFS*, wettability becomes an important concern. Furthermore, most of the *LFS* alloys have good mechanical properties when tested in bulk but their wetting, when soldered on boards, is not good for the reliability of solder joint. This means that wettability or solderability is necessary for characterizing the solder alloys and becomes important when high solder joint's reliability is required (Sadiq, 2012).

There are two well-known tests used to characterize the wettability of solder: Spread area test and wetting balance test (Wu *et al.*, 2004)**.** In the spread area test, the solder disc is coated with flux, melted, and allowed to solidify on a substrate. When a bond is formed, the free energy is reduced and hence the solder changes its shape (Wu *et al.*, 2004). This change in shape causes an increase in the contact area which shows the wetting behaviour of solder. In some cases, the ratio of the as-bonded area to this new area (after soldering) is taken as the wettability of solder (Wu *et al.*, 2004). Wetting balance test is also an important technique to evaluate the solder wettability. In this method, the coupon (for example *Cu*) is dipped into the molten solder present inside the crucible at a temperature more than its *MP*. The molten solder moves up the coupon because of the wetting force exerted on it. Different forces, due to buoyancy,

come in action after partial dipping of the coupon into the solder bath including the surface tensions which are quite high at the solder/flux interface. The resultant force is then the measurement of the meniscus and the wetting angle (Sadiq, 2012).

In a series of investigations for the improvement of wettability of *SAC*, the addition of *RE* elements is the most noticeable (Xiong and Zhang, 2019). The wetting properties of *SAC* and *SAC-La* at 250 °C were investigated by (Sadiq, 2012). It was noticed that the surface tension of *SAC* decreased due to *La* doping. The wetting force of *SAC* was found 5.7 mN which increased up to 6.7 mN for *SAC-0.25La* as shown in Figure 5 (a). However, when the contents of *La* increased to 0.5wt%, the wetting force shows a lower value than *SAC-0.25La.* This concluded that the addition of *La* in *SAC* beyond 0.25 wt% decrease the wetting force which ultimately affects the wettability. Therefore, the optimum composition of *La* in *SAC* should be considered as 0.25 wt%. In the same study, wetting or contact angle were found on the basis of the surface tensions. An appreciable decrease in contact angles was noted with *SAC-0.25La* having a better (smaller) contact angle than *SAC* and *SAC-0.5La* alloys. Figure 5 (b) shows that *SAC-0.25La* decrease the wetting angle of *SAC* from 47° up to 42° and again *SAC-0.5La* show larger wetting angle than *SAC-0.25La*. Therefore, optimum doping of *La* for *SAC* is 0.25 wt%, as beyond this the wetting angle increases which ultimately affects the wettability.

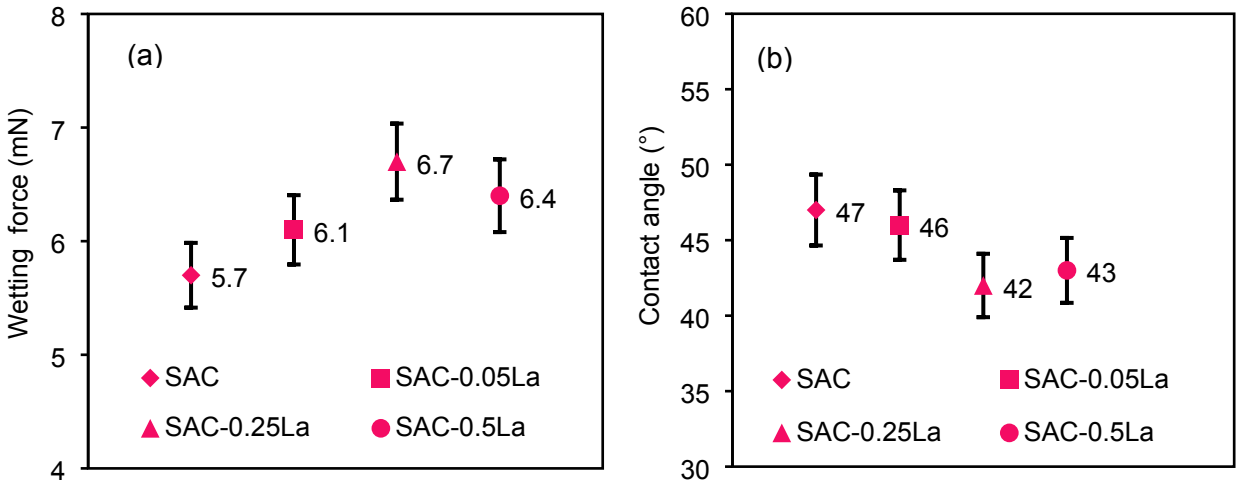

Figure 5: *SAC* and *SAC-La* at 250°C (a) wetting forces, (b) contact angles (Sadiq, 2012)

(Gao *et al.*, 2010a) concluded in their study that trace amounts of *Nd* remarkably improved the wetting behaviour of *SAC*. Figures 6 (a) and 6 (b) show the wetting time and wetting force of *SAC-Nd* at different temperatures which clearly shows that wettability of *SAC* is improved with 0.05 wt% compositions of *Nd* because of its lower surface tension. (Gao *et al.*, 2010b) in another study have also reported that the contents of 0.05 wt% of *Pr* improved the wetting property of *SAC*. Figure 7 shows that the highest spreading area is 63.27 mm which is observed at *SAC-0.05Pr.*

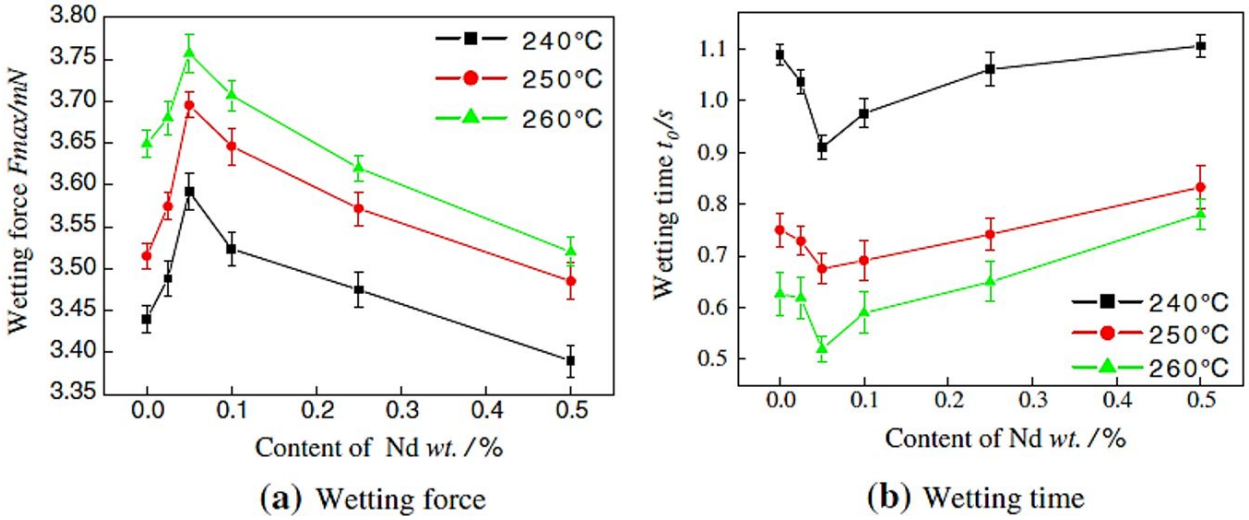

Figure 6: Effect of *Nd* on the solderability of *SAC* solders (Gao *et al.*, 2010a)

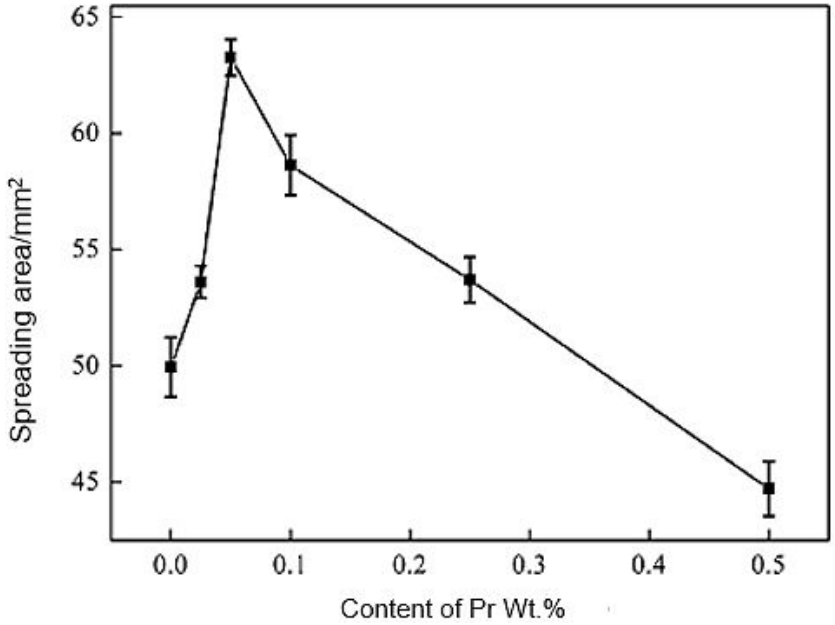

Figure 7: Effect of *Pr* on the solderability of *SAC* (Gao *et al.*, 2010b)

Furthermore, the wettability of *SAC-Ce* was studied by (Jian-Xin Wang *et al.*, 2009). They concluded that after the addition of *Ce*, the wetting behaviour of *SAC* improves significantly. The observed wetting time was ~0.7s at 250 °C, which was very close to that of *Sn-Pb* solder.

Nanoparticles also contribute to improving the overall performance of *SAC*. (Tay *et al.*, 2013) concluded that adding *Ni* nanoparticles into *SAC* increased the wetting angle from 19.3° to 29.9°. (Yoon *et al.*, 2005)also reported that *Co* nanoparticles in *SAC* increased the wetting angle, but decreased the spreading rate. Similar effects with the *Co* nanoparticles were reported by (Haseeb and Leng, 2011). (Tsao *et al.*, 2010) found that 0.5 wt% of Al_2O_3 nanoparticles have the same effect on the wetting behaviour of *SAC*, giving the minimum contact angle of 28.9°. (Yi Li *et al.*, 2014) produced mechanically mixed TiO_2 nanoparticles in *SAC.* Their study showed that adding 0.25 wt% of TiO_2 nanoparticles

decreased the wetting time by 53.7% while the wetting force increased to 37.6%. (Kanlayasiri and Meesathien, 2018) recommended that maximum wettability of *SAC* is achieved at 0.25 wt% of Zinc oxide (*ZnO)* nanoparticles. (Jung *et al.*, 2018) worked on different compositions of TiO_2 and Graphene. All compositions were mixed simultaneously at equal weight fractions into *SAC* molten solder by mechanical mixing method and melteing to produce a bulk nanocomposite solder. Their results showed that nanomaterials with 0.21 wt% had an improved wettability and spreadability by 33.67% and 8.66%, respectively.

6. Conclusions

Lead-free solder alloys are considered to be one of the most important segments of the global green environment. The most commonly used lead-free solder alloy is the Tin-Silver-Copper having good mechanical properties in comparison to the conventional Tin-Lead. Addition of alloying elements or composite approach can overcome limitations of Tin-Silver-Copper solders, especially the microstructure, mechanical properties, and wettability. However, no significant effect on the melting point was observed and thus, no adjustment should be required in the reflow process to meet the requirement of the present soldering process. However, further research is required to ensure that the addition of alloying elements or composite approach can decrease the melting point of Tin-Silver-Copper. Moreover, it is worth noting that the addition of the fourth elements or nanoparticles are actively involved in the contribution of refining the microstructures, giving good mechanical properties and wettability with the condition that the added compositions should not be in the excess amount for the solder joint's reliability. In this regard, developing new lead-free solder alloys during its operating life, the optimum concentration of the alloying element, composite approach or nanoparticles to Tin-Silver-Copper should be examined carefully.

Future studies should investigate the optimal compositions into Tin-Silver-Copper which can improve the thermal behaviour, interfacial reactions, Tin whiskers, wettability, microstructure and, mechanical properties. Moreover, the work should also be extended to get the desired inclusions into Tin-Silver-Copper which can effectively perform better under different strain rates and, thermal ageing at different times and temperatures.

References

Aamir, M.,Muhammad, R.,Ahmed, N. and Alam, K. (2015), "Impact of thermal aging on microstructure and mechanical properties of high Sn content, Sn-Pb solders", *in Fourth International Conference on Aerospace Science & Engineering, Islamabad, Pakistan, Institute of Space Technology*, 2015, *Islamabad, Pakistan*, Institute of Space Technology, pp. 187-191.

Aamir, M.,Muhammad, R.,Ahmed, N.,Sadiq, M.,Waqas, M. and ., I. (2017a), "Mechanical Properties of Lead Free Solder Alloy for Green Electronics under High Strain Rate and Thermal Aging". *Journal of Engineering and Applied Sciences (JEAS), University of Engineering and Technology, Peshawar,* Vol. 36**,** PP. 115-123.

Aamir, M.,Muhammad, R.,Ahmed, N. and Waqas, M. (2017b), "Impact of thermal aging on the intermetallic compound particle size and mechanical properties of lead free solder for green electronics". *Microelectronics Reliability,* Vol. 78**,** PP. 311-318.

Aamir, M., Tolouei-Rad, Majid, Din Israr, Ud, Giasin, Khaled, and Vafadar, A. (2019), "Performance of SAC305 and SAC305-0.4La lead free electronic solders at high temperature". *Soldering & Surface Mount Technology,* Vol. 31**,** PP. 250-260.

Aamir, M.,Waqas, M.,Iqbal, M.,Hanif, M. I. and Muhammad, R. (2017c), "Fuzzy logic approach for investigation of microstructure and mechanical properties of Sn96.5-Ag3.0-Cu0.5 lead free solder alloy". *Soldering & Surface Mount Technology,* Vol. 29**,** PP. 191-198.

Abtew, M. and Selvaduray, G. (2000), "Lead-free solders in microelectronics". *Materials Science and Engineering: R: Reports,* Vol. 27**,** PP. 95-141.

Ali, B. (2015), "Advancement in microstructure and mechanical properties of lanthanum-doped tin-silver-copper lead free solders by optimizing the lanthanum doping concentration". *Soldering & Surface Mount Technology,* Vol. 27**,** PP. 69-75.

Basak, A.,Pramanik, A.,Riazi, H.,Silakhori, M. and Netting, A. (2018), "Development of Pb-Free Nanocomposite Solder Alloys". *Journal of Composites Science,* Vol. 2**,** PP. 28.

Bashir, M. N.,Haseeb, A.,Rahman, A. Z. M. S. and Fazal, M. (2016), "Effect of cobalt doping on the microstructure and tensile properties of lead free solder joint subjected to electromigration". *Journal of Materials Science & Technology,* Vol. 32**,** PP. 1129-1136.

Chang, S.,Jain, C.,Chuang, T.,Feng, L. and Tsao, L. (2011), "Effect of addition of TiO_2 nanoparticles on the microstructure, microhardness and interfacial reactions of Sn3.5AgXCu solder". *Materials & Design,* Vol. 32**,** PP. 4720-4727.

Che, F.,Zhu, W.,Poh, E. S.,Zhang, X. and Zhang, X. (2010), "The study of mechanical properties of Sn–Ag–Cu lead-free solders with different Ag contents and Ni doping under different strain rates and temperatures". *Journal of Alloys and Compounds,* Vol. 507**,** PP. 215-224.

Chen, B. and Li, G. (2004), "Influence of Sb on IMC growth in Sn–Ag–Cu–Sb Pb-free solder joints in reflow process". *Thin Solid Films,* Vol. 462**,** PP. 395-401.

Chen, W.,Kong, J. and Chen, W. (2011), "Effect of rare earth Ce on the microstructure, physical properties and thermal stability of a new lead-free solder". *Journal of Mining and Metallurgy B: Metallurgy,* Vol. 47**,** PP. 11-21.

Cheng, S.,Huang, C.-M. and Pecht, M. (2017), "A review of lead-free solders for electronics applications". *Microelectronics Reliability,* Vol. 75**,** PP. 77-95.

Chuang, C.,Tsao, L.,Lin, H. and Feng, L. (2012), "Effects of small amount of active Ti element additions on microstructure and property of Sn3.5Ag0.5Cu solder". *Materials Science and Engineering: A,* Vol. 558**,** PP. 478-484.

Dharma, I. G. B. B.,Shukor, M. H. A. and Ariga, T. (2009), "Wettability of low silver content lead-free solder alloy". *Materials Transactions,* Vol. 50**,** PP. 1135-1138.

Dudek, M. and Chawla, N. (2010), "Effect of rare-earth (La, Ce, and Y) additions on the microstructure and mechanical behavior of Sn-3.9Ag-0.7Cu solder alloy". *Metallurgical and Materials Transactions A,* Vol. 41**,** PP. 610-620.

Efzan, E. and Marini, A. (2012), "A review of solder evolution in electronic application". *International Journal of Engineering,* Vol. 1**,** PP. 2305-8269.

Efzan Mhd Noor, E.,Singh, A. and Tze Chuan, Y. (2013), "A review: influence of nano particles reinforced on solder alloy". *Soldering & Surface Mount Technology,* Vol. 25**,** PP. 229-241.

El-Daly, A. and El-Taher, A. (2013), "Improved strength of Ni and Zn-doped Sn–2.0Ag–0.5Cu lead-free solder alloys under controlled processing parameters". *Materials & Design,* Vol. 47**,** PP. 607-614.

El-Daly, A. and Hammad, A. (2012), "Enhancement of creep resistance and thermal behavior of eutectic Sn–Cu lead-free solder alloy by Ag and In-additions". *Materials & Design,* Vol. 40**,** PP. 292-298.

El-Daly, A.,Hammad, A.,Fawzy, A. and Nasrallh, D. (2013), "Microstructure, mechanical properties, and deformation behavior of Sn–1.0Ag–0.5Cu solder after Ni and Sb additions". *Materials & Design,* Vol. 43**,** PP. 40-49.

Fallahi, H.,Nurulakmal, M.,Arezodar, A. F. and Abdullah, J. (2012), "Effect of iron and indium on IMC formation and mechanical properties of lead-free solder". *Materials Science and Engineering: A,* Vol. 553**,** PP. 22-31.

Gain, A. K.,Chan, Y. C. and Yung, W. K. (2011), "Microstructure, thermal analysis and hardness of a Sn–Ag–Cu–1wt% nano-TiO_2 composite solder on flexible ball grid array substrates". *Microelectronics Reliability,* Vol. 51**,** PP. 975-984.

Gain, A. K.,Fouzder, T.,Chan, Y. C.,Sharif, A.,Wong, N. B. and Yung, W. K. (2010), "The influence of addition of Al nano-particles on the microstructure and shear strength of eutectic Sn–Ag–Cu solder on Au/Ni metallized Cu pads". *Journal of Alloys and Compounds,* Vol. 506**,** PP. 216-223.

Gain, A. K. and Zhang, L. (2019), "Effects of Ni nanoparticles addition on the microstructure, electrical and mechanical properties of Sn-Ag-Cu alloy". *Materialia,* Vol. 5**,** PP. 100234.

Gain, A. K. and Zhang, L. (2018), "The effects of TiO_2 nanoparticles addition on the thermal shock resistance, shear strength and IMC layer growth of SAC305 alloy". *Materialia,* Vol. 3**,** PP. 64-73.

Gao, L.,Xue, S.,Zhang, L.,Sheng, Z.,Zeng, G. and Ji, F. (2010a), "Effects of trace rare earth Nd addition on microstructure and properties of SnAgCu solder". *Journal of Materials Science: Materials in Electronics,* Vol. 21**,** PP. 643-648.

Gao, L.,Xue, S.,Zhang, L.,Xiao, Z.,Dai, W.,Ji, F.,Ye, H. and Zeng, G. (2010b), "Effect of praseodymium on the microstructure and properties of Sn3.8Ag0.7Cu solder". *Journal of Materials Science: Materials in Electronics,* Vol. 21**,** PP. 910-916.

Hammad, A. (2018), "Enhancing the ductility and mechanical behavior of Sn-1.0Ag-0.5Cu lead-free solder by adding trace amount of elements Ni and Sb". *Microelectronics Reliability,* Vol. 87**,** PP. 133-141.

Hammad, A. (2013), "Evolution of microstructure, thermal and creep properties of Ni-doped Sn–0.5Ag–0.7Cu low-Ag solder alloys for electronic applications". *Materials & Design,* Vol. 52**,** PP. 663-670.

Hao, H.,Tian, J.,Shi, Y.,Lei, Y. and Xia, Z. (2007), "Properties of Sn3.8Ag0.7Cu solder alloy with trace rare earth element Y additions". *Journal of electronic materials,* Vol. 36**,** PP. 766-774.

Harrison, M.,Vincent, J. and Steen, H. (2001), "Lead-free reflow soldering for electronics assembly". *Soldering & Surface Mount Technology,* Vol. 13**,** PP. 21-38.

Haseeb, A.,Arafat, M.,Tay, S. and Leong, Y. (2017), "Effects of metallic nanoparticles on interfacial intermetallic compounds in tin-based solders for microelectronic packaging". *Journal of electronic materials,* Vol. 46**,** PP. 5503-5518.

Haseeb, A. and Leng, T. S. (2011), "Effects of Co nanoparticle addition to Sn–3.8Ag–0.7Cu solder on interfacial structure after reflow and ageing". *Intermetallics,* Vol. 19**,** PP. 707-712.

Huang, M. and Wang, L. (2005), "Effects of Cu, Bi, and In on microstructure and tensile properties of Sn-Ag-X (Cu, Bi, In) solders". *Metallurgical and Materials Transactions A,* Vol. 36**,** PP. 1439-1446.

Jeon, S.-j.,Hyun, S.,Lee, H.-J.,Kim, J.-W.,Ha, S.-S.,Yoon, J.-W.,Jung, S.-B. and Lee, H.-J. (2008), "Mechanical reliability evaluation of Sn-37Pb solder joint using high speed lap-shear test". *Microelectronic Engineering,* Vol. 85**,** PP. 1967-1970.

Jung, D.-H.,Sharma, A. and Jung, J.-P. (2018), "Influence of dual ceramic nanomaterials on the solderability and interfacial reactions between lead-free Sn-Ag-Cu and a Cu conductor". *Journal of Alloys and Compounds,* Vol. 743**,** PP. 300-313.

Kanlayasiri, K. and Meesathien, N. (2018), "Effects of Zinc Oxide Nanoparticles on Properties of SAC0307 Lead-Free Solder Paste". *Advances in Materials Science and Engineering,* Vol. 2018**,** PP. 1-10.

Kanlayasiri, K.,Mongkolwongrojn, M. and Ariga, T. (2009), "Influence of indium addition on characteristics of Sn–0.3Ag–0.7Cu solder alloy". *Journal of Alloys and Compounds,* Vol. 485**,** PP. 225-230.

Kumar, K. M.,Kripesh, V. and Tay, A. A. (2008), "Single-wall carbon nanotube (SWCNT) functionalized Sn–Ag–Cu lead-free composite solders". *Journal of Alloys and Compounds,* Vol. 450**,** PP. 229-237.

Lee, N.-C. (1997), "Getting ready for lead-free solders". *Soldering & Surface Mount Technology,* Vol. 9**,** PP. 65-69.

Leong, Y. and Haseeb, A. (2016), "Soldering characteristics and mechanical properties of Sn-1.0Ag-0.5Cu solder with minor aluminum addition". *Materials,* Vol. 9**,** PP. 522.

Li, G.,Chen, B.,Shi, X.,Wong, S. C. and Wang, Z. (2006), "Effects of Sb addition on tensile strength of Sn–3.5Ag–0.7Cu solder alloy and joint". *Thin Solid Films,* Vol. 504**,** PP. 421-425.

Li, Y.,Zhao, X.,Liu, Y.,Wang, Y. and Wang, Y. (2014), "Effect of TiO_2 addition concentration on the wettability and intermetallic compounds growth of Sn3.0Ag0.5Cu–xTiO_2 nano-composite solders". *Journal of Materials Science: Materials in Electronics,* Vol. 25**,** PP. 3816-3827.

Liang, J.,Luo, T.,Hu, A. and Li, M. (2014), "Formation and growth of interfacial intermetallic layers of Sn–8Zn–3Bi–0.3Cr on Cu, Ni and Ni–W substrates". *Microelectronics Reliability,* Vol. 54**,** PP. 245-251.

Liu, P.,Yao, P. and Liu, J. (2008), "Effect of SiC nanoparticle additions on microstructure and microhardness of Sn-Ag-Cu solder alloy". *Journal of electronic materials,* Vol. 37**,** PP. 874-879.

Liu, X.,Han, Y.,Jing, H.,Wei, J. and Xu, L. (2013), "Effect of graphene nanosheets reinforcement on the performance of SnAgCu lead-free solder". *Materials Science and Engineering: A,* Vol. 562**,** PP. 25-32.

Luo, D.-x.,Xue, S.-b. and Li, Z.-q. (2014), "Effects of Ga addition on microstructure and properties of Sn–0.5 Ag–0.7 Cu solder". *Journal of Materials Science: Materials in Electronics,* Vol. 25**,** PP. 3566-3571.

Ma, H. and Suhling, J. C. (2009), "A review of mechanical properties of lead-free solders for electronic packaging". *Journal of materials science,* Vol. 44**,** PP. 1141-1158.

Mei, Z.,Holder, H. A. and Vander Plas, H. A. (1996), "Low-temperature solders". *Hewlett Packard Journal,* Vol. 47**,** PP. 91-98.

Nai, S.,Wei, J. and Gupta, M. (2008), "Effect of carbon nanotubes on the shear strength and electrical resistivity of a lead-free solder". *Journal of electronic materials,* Vol. 37**,** PP. 515-522.

Nai, S.,Wei, J. and Gupta, M. (2006), "Influence of ceramic reinforcements on the wettability and mechanical properties of novel lead-free solder composites". *Thin Solid Films,* Vol. 504**,** PP. 401-404.

Nimmo, K. (2004), "Alloy selections". *Lead-Free Soldering in Electronics—Science, Technology and Environmental Impact,* Vol.**,** PP. 49-90.

Roshanghias, A.,Kokabi, A.,Miyashita, Y.,Mutoh, Y.,Rezayat, M. and Madaah-Hosseini, H. (2012), "Ceria reinforced nanocomposite solder foils fabricated by accumulative roll bonding process". *Journal of Materials Science: Materials in Electronics,* Vol. 23**,** PP. 1698-1704.

Sabri, M. F. M.,Shnawah, D. A.,Badruddin, I. A.,Said, S. B. M.,Che, F. X. and Ariga, T. (2013), "Microstructural stability of Sn–1Ag–0.5 Cu–xAl (x= 1, 1.5, and 2wt.%) solder alloys and the effects of high-temperature aging on their mechanical properties". *Materials Characterization,* Vol. 78**,** PP. 129-143.

Sadiq, M. (2012). "Design and fabrication of lanthanum-doped Sn-Ag-Cu lead-free solder for next generation microelectronics applications in severe environment". *Doctoral dissertation,* Georgia Institute of Technology.

Sadiq, M.,Pesci, R. and Cherkaoui, M. (2013), "Impact of thermal aging on the microstructure evolution and mechanical properties of lanthanum-doped tin-silver-copper lead-free solders". *Journal of electronic materials,* Vol. 42**,** PP. 492-501.

Sharma, A.,Yu, H.,Cho, I. S.,Seo, H. and Ahn, B. (2019), "ZrO_2 nanoparticle embedded low silver lead free solder alloy for modern electronic devices". *Electronic Materials Letters,* Vol. 15**,** PP. 27-35.

Shi, Y.,Tian, J.,Hao, H.,Xia, Z.,Lei, Y. and Guo, F. (2008), "Effects of small amount addition of rare earth Er on microstructure and property of SnAgCu solder". *Journal of Alloys and Compounds,* Vol. 453**,** PP. 180-184.

Shnawah, D. A.,Sabri, M. F. M. and Badruddin, I. A. (2012), "A review on thermal cycling and drop impact reliability of SAC solder joint in portable electronic products". *Microelectronics Reliability,* Vol. 52**,** PP. 90-99.

Shnawah, D. A.,Sabri, M. F. M.,Badruddin, I. A.,Said, S. B. M.,Ariga, T. and Che, F. X. (2013), "Effect of Ag content and the minor alloying element Fe on the mechanical properties and microstructural stability of Sn-Ag-Cu solder alloy under high-temperature annealing". *Journal of electronic materials,* Vol. 42**,** PP. 470-484.

Sona, M. and Prabhu, K. (2013), "Review on microstructure evolution in Sn–Ag–Cu solders and its effect on mechanical integrity of solder joints". *Journal of Materials Science: Materials in Electronics,* Vol. 24**,** PP. 3149-3169.

Sujan, G.,Haseeb, A.,Nishikawa, H. and Amalina, M. (2017), "Interfacial reaction, ball shear strength and fracture surface analysis of lead-free solder joints prepared using cobalt nanoparticle doped flux". *Journal of Alloys and Compounds,* Vol. 695**,** PP. 981-990.

Sun, L. and Zhang, L. (2015), "Properties and microstructures of Sn-Ag-Cu-X lead-free solder joints in electronic packaging". *Advances in Materials Science and Engineering,* Vol. 2015**,** PP. 16.

Tang, Y.,Li, G. and Pan, Y. (2014), "Effects of TiO_2 nanoparticles addition on microstructure, microhardness and tensile properties of Sn–3.0Ag–0.5Cu–xTiO_2 composite solder". *Materials & Design,* Vol. 55**,** PP. 574-582.

Tay, S.,Haseeb, A.,Johan, M. R.,Munroe, P. and Quadir, M. Z. (2013), "Influence of Ni nanoparticle on the morphology and growth of interfacial intermetallic compounds between Sn–3.8Ag–0.7Cu lead-free solder and copper substrate". *Intermetallics,* Vol. 33**,** PP. 8-15.

Tsao, L.,Chang, S.,Lee, C.,Sun, W. and Huang, C. (2010), "Effects of nano-Al_2O_3 additions on microstructure development and hardness of Sn3.5Ag0.5Cu solder". *Materials & Design,* Vol. 31**,** PP. 4831-4835.

Tsao, L.,Wu, R.,Cheng, T.-H.,Fan, K.-H. and Chen, R. (2013), "Effects of nano-Al_2O_3 particles on microstructure and mechanical properties of Sn3.5Ag0.5Cu composite solder ball grid array joints on Sn/Cu pads". *Materials & Design,* Vol. 50**,** PP. 774-781.

Tu, X.,Yi, D.,Wu, J. and Wang, B. (2017), "Influence of Ce addition on Sn-3.0Ag-0.5Cu solder joints: Thermal behavior, microstructure and mechanical properties". *Journal of Alloys and Compounds,* Vol. 698**,** PP. 317-328.

Vianco, P. and Shangguan, D. (2006), "Fatigue and creep of lead-free solder alloys: fundamental properties, chapter 3, Leadfree solder interconnect reliability". *ASM International, Materials Park, OH,* Vol.**,** PP. 67-106.

Wang, H.,Lu, T.,Yi, D. and Wang, B. (2019), "Microstructure refinement, characterization of tensile behavior and aging resistance of Zr-modified SAC105 solder alloy". *Journal of Materials Science: Materials in Electronics,* Vol. 30**,** PP. 11429–11439.

Wang, J.-X.,Xue, S.-B.,Han, Z.-J.,Yu, S.-L.,Chen, Y.,Shi, Y.-P. and Wang, H. (2009), "Effects of rare earth Ce on microstructures, solderability of Sn–Ag–Cu and Sn–Cu–Ni solders as well as mechanical properties of soldered joints". *Journal of Alloys and Compounds,* Vol. 467**,** PP. 219-226.

Wu, C. and Wong, Y. (2007), "Rare-earth additions to lead-free electronic solders". *Journal of Materials Science: Materials in Electronics,* Vol. 18**,** PP. 77-91.

Wu, C.,Yu, D.,Law, C. and Wang, L. (2004), "Properties of lead-free solder alloys with rare earth element additions". *Materials Science and Engineering: R: Reports,* Vol. 44**,** PP. 1-44.

Xia, Z.,Chen, Z.,Shi, Y.,Mu, N. and Sun, N. (2002), "Effect of rare earth element additions on the microstructure and mechanical properties of tin-silver-bismuth solder". *Journal of electronic materials,* Vol. 31**,** PP. 564-567.

Xiong, M.-y. and Zhang, L. (2019), "Interface reaction and intermetallic compound growth behavior of Sn-Ag-Cu lead-free solder joints on different substrates in electronic packaging". *Journal of materials science,* Vol. 54**,** PP. 1741-1768.

Xu, L.,Wang, L.,Jing, H.,Liu, X.,Wei, J. and Han, Y. (2015), "Effects of graphene nanosheets on interfacial reaction of Sn–Ag–Cu solder joints". *Journal of Alloys and Compounds,* Vol. 650**,** PP. 475-481.

Yakymovych, A.,Plevachuk, Y.,Sklyarchuk, V.,Sokoliuk, B.,Galya, T. and Ipser, H. (2017), "Microstructure and electro-physical properties of Sn-3.0Ag-0.5Cu nanocomposite solder reinforced with Ni nanoparticles in the melting-solidification temperature range". *Journal of Phase Equilibria and Diffusion,* Vol. 38**,** PP. 217-222.

Yang, Z.,Zhou, W. and Wu, P. (2014), "Effects of Ni-coated carbon nanotubes addition on the microstructure and mechanical properties of Sn–Ag–Cu solder alloys". *Materials Science and Engineering: A,* Vol. 590**,** PP. 295-300.

Yasmin, T. and Sadiq, M. (2014), "Impact of lanthanum doping on SAC305 lead free solders for high temperature applications". *Journal of Engineering and Applied Sciences (JEAS), University of Engineering and Technology, Peshawar,* Vol. 33**,** PP. 29-36.

Yoon, J.-W.,Kim, S.-W. and Jung, S.-B. (2005), "IMC morphology, interfacial reaction and joint reliability of Pb-free Sn–Ag–Cu solder on electrolytic Ni BGA substrate". *Journal of Alloys and Compounds,* Vol. 392**,** PP. 247-252.

Zhang, L.,Fan, X.-y.,Guo, Y.-h. and He, C.-w. (2014), "Properties enhancement of SnAgCu solders containing rare earth Yb". *Materials & Design,* Vol. 57**,** PP. 646-651.

Zhang, L.,Han, J.-g.,He, C.-w. and Guo, Y.-h. (2012a), "Effect of Zn on properties and microstructure of SnAgCu alloy". *Journal of Materials Science: Materials in Electronics,* Vol. 23**,** PP. 1950-1956.

Zhang, L.,Xue, S. B.,Zeng, G.,Gao, L. L. and Ye, H. (2012b), "Interface reaction between SnAgCu/SnAgCuCe solders and Cu substrate subjected to thermal cycling and isothermal aging". *Journal of Alloys and Compounds,* Vol. 510**,** PP. 38-45.

Zhu, Z.,Chan, Y.-C.,Chen, Z.,Gan, C.-L. and Wu, F. (2018), "Effect of the size of carbon nanotubes (CNTs) on the microstructure and mechanical strength of CNTs-doped composite Sn0.3Ag0.7Cu-CNTs solder". *Materials Science and Engineering: A,* Vol. 727**,** PP. 160-169.

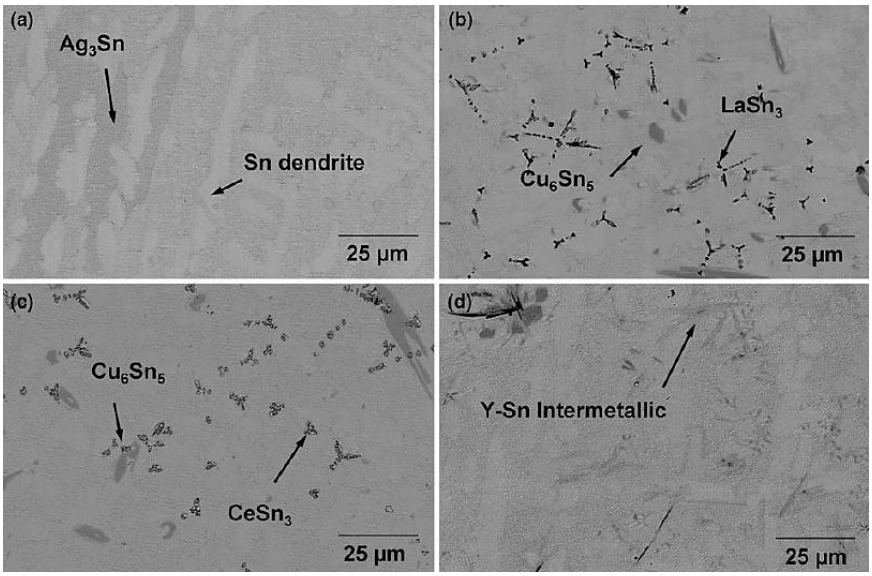

Figure 1: *SEM* micrographs of (a) *SAC* with the addition of 0.5 wt% of (b) *La* (c) *Ce* and (d) *Y* (Dudek and Chawla, 2010)

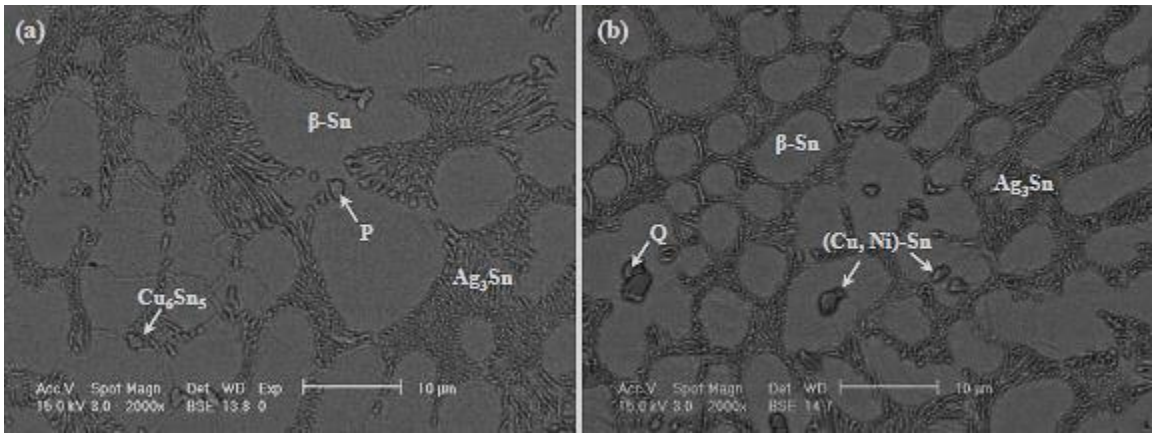

Figure 2: *SEM* images of (a) *SAC* and (b) SAC-0.5wt% nanosized *Ni* particles (Gain and Zhang, 2019)

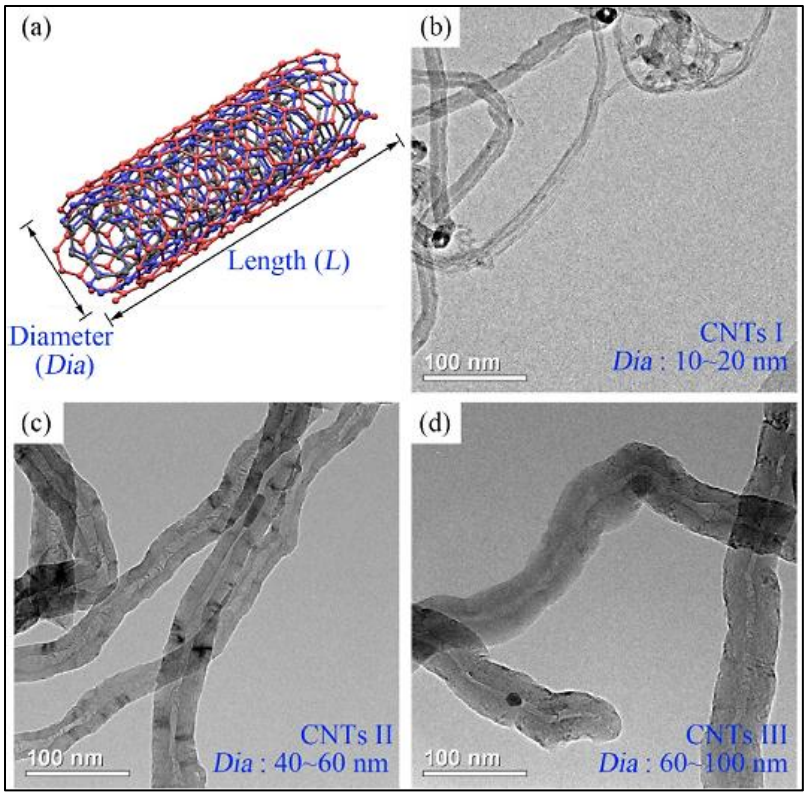

Figure 3: (a) Schematic diagram of *MWCNTs* structure, and *TEM* images of *CNTs*: (b) 10~20 (c) 40~60nm (d) 60~100 (Zhu *et al.*, 2018).

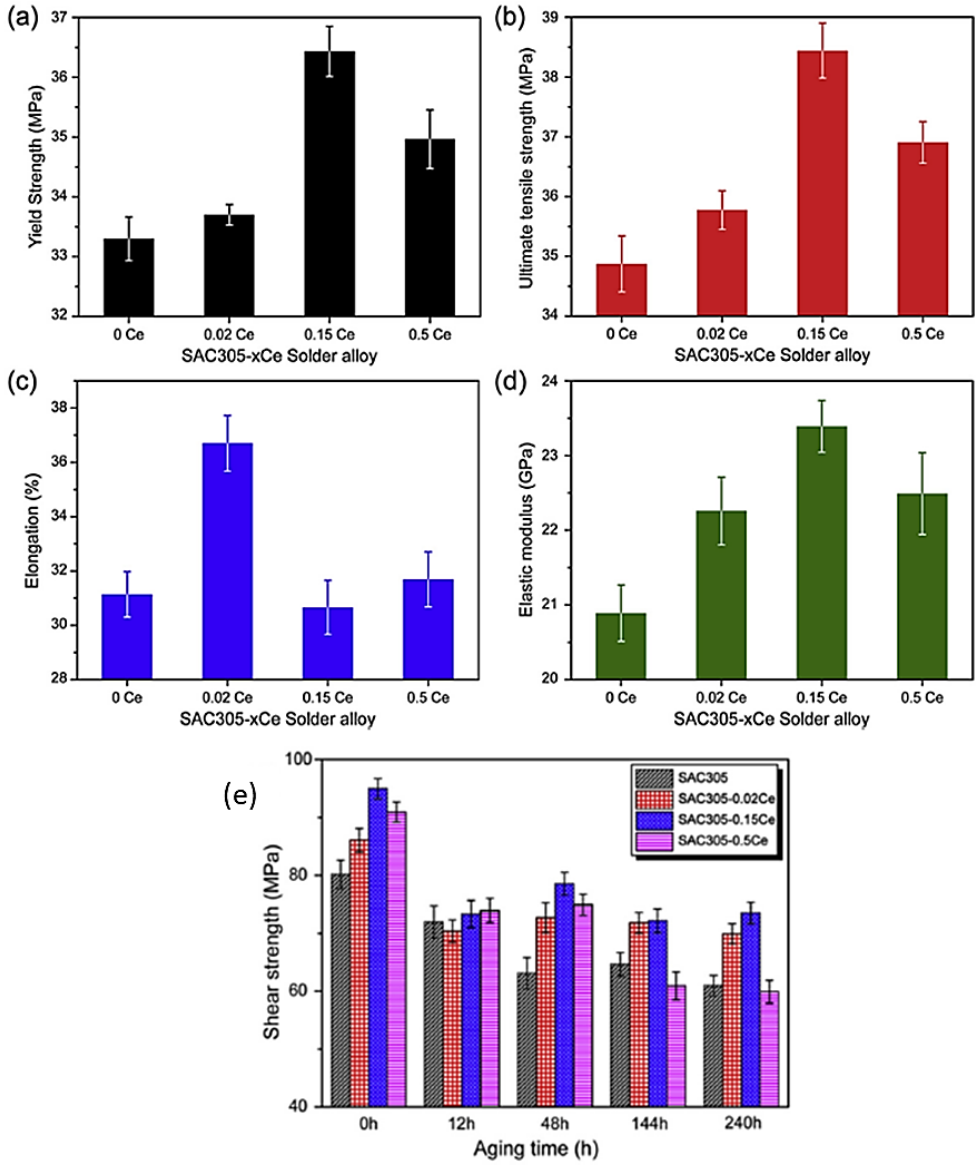

Figure 4: Mechanical properties of the *SAC* with different compositions of *Ce* (Tu *et al.*, 2017)

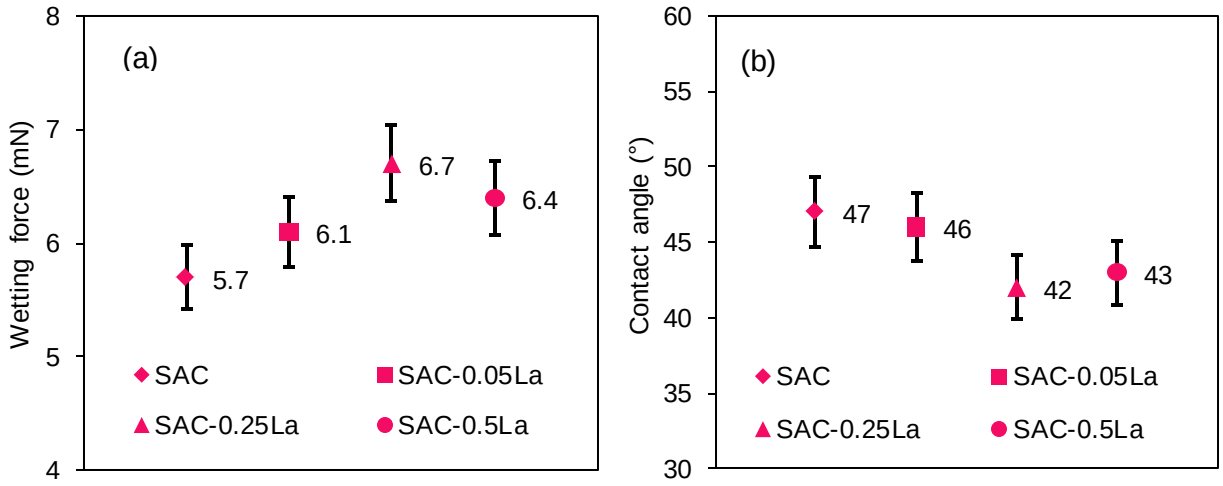

Figure 5: *SAC* and *SAC-La* at 250°C (a) wetting forces, (b) contact angles (Sadiq, 2012)

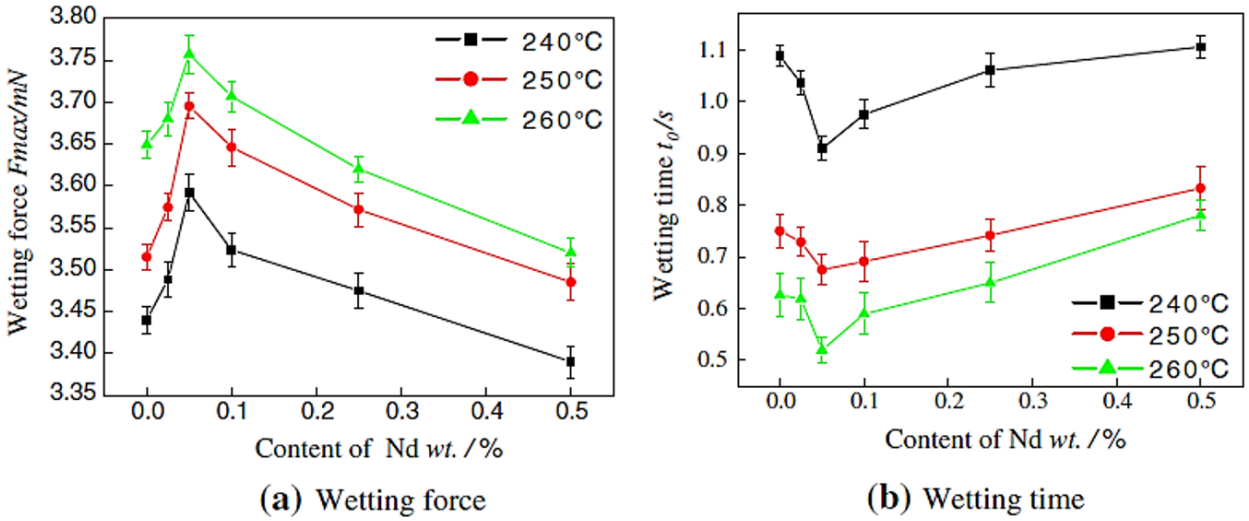

Figure 6: Effect of *Nd* on the solderability of *SAC* solders (Gao *et al.*, 2010a)

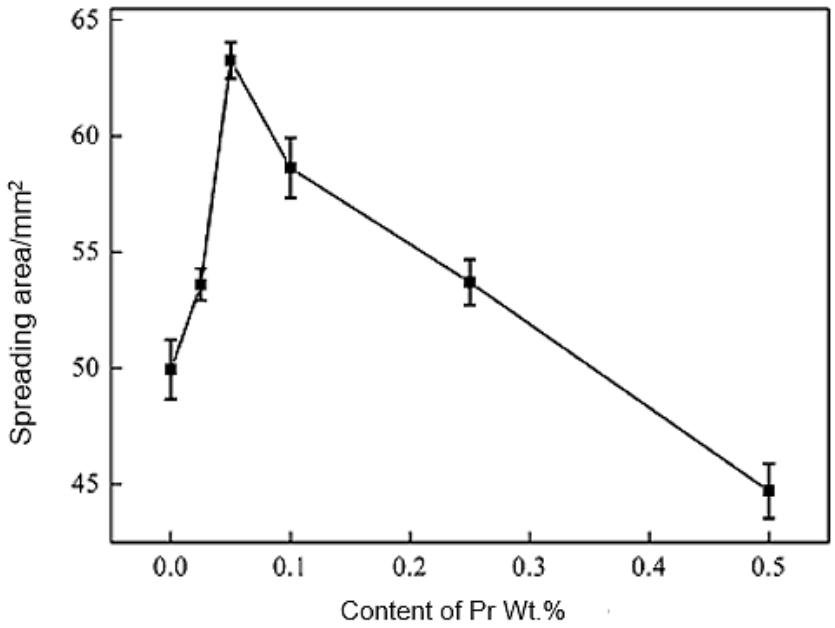

Figure 7: Effect of *Pr* on the solderability of *SAC* (Gao *et al.*, 2010b)

Table 1: Role of the fourth element in the mechanical properties of *SAC*

Alloying element	Composition wt%	Mechanical properties	References
Ti	Up to 1.0 wt%	Increase the *YS, UTS,* and microhardness of *SAC*	(Chuang *et al.*, 2012)
Fe	0.6 wt%	Shear strength of *SAC* increases up to 53 MPa from 29 MPa	(Fallahi *et al.*, 2012)
Zn	0.8 wt%	Improves the tensile force of *the SAC* joint by 10%.	(Zhang *et al.*, 2012a)
Ni	0.5 wt%	Improves *YS*, *UTS,* and ductility of *SAC*	(El-Daly and El-Taher, 2013)
Sb	0.5 wt%	Gives higher strength and ductility	(Hammad, 2018)
Ga	Up to 0.5 wt%	Improves the shear strength of *SAC* solder joint up to 17.9%	(Luo *et al.*, 2014)
La	0.3 wt%	Increase in *YS*, *UTS*, and ductility are found which then improve toughness, creep and fatigue resistance of the *SAC*	(Ali, 2015)
Y	<0.15 wt%	The strength of the *SAC* joint is improved	(Hao *et al.*, 2007)
Er	≤0.1 wt%	Shear strength of *SAC* solder is improved by 18%	(Shi *et al.*, 2008)
Nd	0.05 wt %	Pull force and shear force of *SAC* joint are increased by 19.4% and 23.6%, respectively	(Gao *et al.*, 2010a)
Pr	0.05 wt%	Improves pull force and shear force of *SAC* solder	(Gao *et al.*, 2010b)
Yb	Up to 0.05 wt%	The tensile force of the *SAC* solder joint increase by 25.4%	(Zhang *et al.*, 2014)
Ce	0.15 wt%	Increase the shear strength, ductility, *E, YS,* and *UTS*	(Tu *et al.*, 2017)
Al Nanoparticles	3.0 wt%	Improves the shear strength of *SAC*	(Gain *et al.*, 2010)
Al_2O_3 *Nanoparticles*	1.0 wt%	The shear strength after 1 cycle and 8 cycles of reflow is increase by 14.4% and 16.5%	(Tsao *et al.*, 2013)
TiO_2 *Nanoparticles*	0.1 wt%	Gives better microhardness and tensile properties	(Tang *et al.*, 2014)
CeO_2 *Nanoparticles*	0.75 wt%	improves *YS* and *UTS* of *SAC*	(Roshanghias *et al.*, 2012)

TiB_2 Nanoparticles	3 vol%	Increase *YS* and *UTS* by 26% and 23%, respectively	(Nai *et al.*, 2006)
Co- nanoparticles	2 wt%	Increase the tensile strength of *SAC*	(Bashir *et al.*, 2016)
Ni- nanoparticles	0.5 wt%	The elastic modulus, shear modulus, and microhardness increase by 8%, 11.2%, and 16.7% in *SAC*, respectively.	(Gain and Zhang, 2019)
Ni-CNTs	0.05 wt%	Improves the tensile strength of *SAC* solder slabs and joints	(Yang *et al.*, 2014)
SWCNT	1.0 wt%	Increase the *UTS* of *SAC* up to 50%	(Kumar *et al.*, 2008)
MWCNT	10-60 nm	Improvement *E, YS* and *UTS* of *SAC* are found	(Zhu *et al.*, 2018)
GNSs	0.03 wt%	Increase the *UTS* of *SAC* solder by approximately 10%	(XD Liu *et al.*, 2013)